

Impact of the anaerobic feeding mode on substrate distribution in aerobic granular sludge

Haaksman, V. A.; Schouteren, M.; van Loosdrecht, M. C.M.; Pronk, M.

10.1016/j.watres.2023.119803

Publication date

Document Version Final published version

Published in Water Research

Citation (APA)

Haaksman, V. A., Schouteren, M., van Loosdrecht, M. C. M., & Pronk, M. (2023). Impact of the anaerobic feeding mode on substrate distribution in aerobic granular sludge. Water Research, 233, Article 119803. https://doi.org/10.1016/j.watres.2023.119803

Important note

To cite this publication, please use the final published version (if applicable). Please check the document version above.

Other than for strictly personal use, it is not permitted to download, forward or distribute the text or part of it, without the consent of the author(s) and/or copyright holder(s), unless the work is under an open content license such as Creative Commons.

Takedown policy

Please contact us and provide details if you believe this document breaches copyrights. We will remove access to the work immediately and investigate your claim.

\$ SUPER

Contents lists available at ScienceDirect

Water Research

journal homepage: www.elsevier.com/locate/watres





Impact of the anaerobic feeding mode on substrate distribution in aerobic granular sludge

V.A. Haaksman^{a,*}, M. Schouteren^a, M.C.M. van Loosdrecht^a, M. Pronk^{a,b}

- a Department of Biotechnology, Faculty of Applied Sciences, Delft University of Technology, Van der Maasweg 9, Delft, 2629 HZ, The Netherlands
- ^b Royal HaskoningDHV, Laan 1914 35, Amersfoort, 3800 AL, The Netherlands

ARTICLE INFO

Keywords: aerobic granular sludge PHA bottom-feeding pulse-feeding anaerobic selector continuous flow

ABSTRACT

There is a growing interest to implement aerobic granular sludge (AGS) in existing conventional activated sludge (CAS) systems with a continuous flow-through configuration. The mode of anaerobic contact of raw sewage with the sludge is an important aspect in the adaptation of CAS systems to accommodate AGS. It remains unclear how the distribution of substrate over the sludge by a conventional anaerobic selector compares to the distribution via bottom-feeding applied in sequencing batch reactors (SBRs). This study investigated the effect of the anaerobic contact mode on the substrate (and storage) distribution by operating two lab-scale SBRs; one with the traditional bottom-feeding through a settled sludge bed similar to full-scale AGS systems, and one where the synthetic wastewater was fed as a pulse at the start of the anaerobic phase while the reactor was mixed through sparging of nitrogen gas (mimicking a plug-flow anaerobic selector in continuous flow-through systems). The distribution of the substrate over the sludge particle population was quantified via PHA analysis, combined with the obtained granule size distribution. Bottom-feeding was found to primarily direct substrate towards the large granular size classes (i.e. large volume and close to the bottom), while completely mixed pulse-feeding gives a more equal distribution of substrate over all granule sizes (i.e. surface area dependant). The anaerobic contact mode directly controls the substrate distribution over the different granule sizes, irrespective of the solids retention time of a granule as an entity. Preferential feeding of the larger granules will enhance and stabilise the granulation compared to pulse-feeding, certainly under less advantageous conditions imposed by real sewage.

1. Introduction

Aerobic granular sludge (AGS) is a novel technology for compact treatment of wastewater, applied mainly in sequencing batch reactors (SBRs) at full-scale (Pronk et al., 2015). There is a growing interest to implement AGS in existing conventional activated sludge (AS) systems, mostly with a continuous flow-through configuration (Kent et al., 2018; Winkler and van Loosdrecht, 2022). The increased settleability of AGS compared to conventional AS would allow for a higher mixed-liquor suspended solids (MLSS) for the same volumetric loading rate, yielding an increase in biological treatment capacity. Simultaneous nutrient removal processes within the biofilms also could be utilized to a larger extent (Strubbe et al., 2022).

For a similar successful implementation of AGS in conventional AS systems, the required selective pressures for the formation and retention of AGS must be translated from the SBRs to continuous flow-through systems. The anaerobic storage of readily biodegradable COD (rbCOD)

as polyhydroxyalkanoates (PHAs) ensures dense growth of heterotrophic biomass during subsequent aeration by preventing transportlimited growth (De Kreuk and Van Loosdrecht, 2004). At full-scale, the fraction of rbCOD in municipal wastewater is often limited and the more slowly biodegradable, especially the particulate COD fraction, has been hypothesized to result in flocculent growth under aerobic conditions (Layer et al., 2019; Pronk et al., 2015). Ensuring that anaerobic storage of the limited rbCOD is performed by the sludge fraction with the highest settling velocity speeds up the formation of granular sludge when starting from a flocculent morphology, and results in a larger mean granule size (van Dijk et al., 2022). The selection criterion for AGS is therefore not only to ensure anaerobic uptake of rbCOD and storage as PHAs, but to concentrate the available rbCOD in the best settling sludge fraction as well (i.e. selective feeding). In bottom-fed sequencing batch reactors, both criteria are automatically achieved since the best-settling granules have a higher probability to accumulate at the bottom of the sludge bed. In other reactor configurations,

E-mail address: v.a.haaksman@tudelft.nl (V.A. Haaksman).

^{*} Corresponding author.

particularly in continuous flow-through reactors, this might be more difficult to achieve.

The method of anaerobic contact of raw sewage with the sludge is an important aspect in the adaptation of continuous flow-through activated sludge systems to accommodate AGS. Continuous activated sludge systems designed for enhanced biological phosphorus removal generally employ a plug-flow anaerobic selector zone in which part of the recycled sludge is contacted with the influent while in suspension (Martins et al., 2004). The applied loading rate (mass of rbCOD/mass of sludge/amount time) aims to minimise diffusion gradients of rbCOD inside the sludge flocs and the sludge loading (mass of rbCOD/mass of sludge) sets the amount of flocs over which the incoming rbCOD is distributed. These parameters respectively determine the initial penetration depth of rbCOD and the total amount of stored COD per sludge particle/floc, resulting in relatively dense and well-settling flocs (Wanner et al., 1987). Since the sludge is kept in suspension, sludge particles with a larger surface area to volume ratio can achieve a higher volumetric rbCOD uptake rate if the penetration depth is limited. This favours a flocculent morphology over a granular morphology. A higher initial concentration gradient of rbCOD (i.e. an increased loading rate) can partially counteract the lower surface to volume ratio of granules compared to flocs due to full penetration of even the largest granules. Whether this can be achieved to such an extent that granules can be formed that are substantially larger than flocs, likely depends on the fraction of rbCOD compared to the total COD in the wastewater (van Dijk et al., 2022).

Some full-scale studies have investigated the relation between the design of an anaerobic selector and the sludge morphology with a focus on aerobic granulation. Redmond et al. (2019) investigated the effect of the sludge settleability of a WWTP which had the flow pattern of the anaerobic selector converted from a tanks-in-series configuration to a step-feed. The characteristics of the sludge settleability were very similar to that of aerobic granular sludge in the tanks-in-series configuration, with a SVI5/SVI30-ratio close to unity. The ratio gradually increased after the transition to a more flocculent morphology in the step-feed configuration. These findings demonstrated the adverse effect of a decrease in initial rbCOD loading and initial rbCOD loading rate on the granular sludge morphology. Wei et al. (2020) investigated the process conditions of several full-scale conventional AS facilities in the USA with varying levels of spontaneous granulation. No correlation was found between the COD loading rate of the anaerobic selector and the level of granulation observed (the rbCOD loading rates were not reported). The level of granulation did correlate strongly with the fraction of phosphate accumulating organisms (PAOs) found in the granular sludge fraction compared to the flocculent fraction, indicative of an increased enrichment for anaerobic uptake of rbCOD in the granular fraction. It remains unclear how the distribution of substrate over the sludge by a conventional anaerobic selector compares to the distribution via bottom-feeding applied in SBRs, and how it impacts the granulation process. The implementation of stable AGS into existing continuous flow-through WWTPs thus requires further study on the impact of the anaerobic contact mode of sewage with sludge.

To investigate the effect of the anaerobic contact mode on the substrate (and storage) distribution, the granulation potential, the size distribution, and related conversions, we operated two lab-scale SBRs; one with the traditional bottom-feeding through a settled sludge bed similar to full-scale AGS systems, and one where the synthetic wastewater was fed as a pulse at the start of the anaerobic phase while the reactor was mixed by sparging of nitrogen gas. The latter generates exposure of the sludge to a high substrate concentration at the start of the anaerobic period, which gradually decreases to zero. From a biological process view this can be considered a scaled down version of a plug-flow anaerobic selector as employed in conventional AS systems. Starting from flocculent sludge, the formation of aerobic granular sludge was followed. The effect of the contact method on the distribution of the substrate over the sludge particle population was quantified via PHA analysis, combined with the granule size distribution. The interactions

between the anaerobic contact mode and aerobic conversion processes were investigated. Implications for application in continuous systems and the nutrient removal process are discussed.

2. Materials and methods

2.1. Reactor set-up and operation

Two cylindrical lab-scale reactors (i.e. one pulse-fed, one bottomfed), each with a working volume of 3 L during aeration and an aspect ratio of 20, were operated as a sequential batch reactor with a volume exchange ratio of 0.47. The reactors were operated continuously in 205 min cycles during 144 days. After settling and discharge of effluent, the working volume of the reactor was 1.6 L. A cycle started with an anaerobic phase in which synthetic wastewater was fed. A different anaerobic contact mode was used in each reactor. The pulse-fed reactor was first sparged with dinitrogen gas (5 min) with 5 L min⁻¹ (superficial gas velocity of 3.5 cm s⁻¹) to deplete the bulk-liquid of dissolved oxygen. The batch of synthetic wastewater was then fed while sparging and mixing continued (2 min). The pulse-fed reactor was subsequently mixed with dinitrogen gas for the remainder of the anaerobic phase (53) min). For the bottom-fed reactor, synthetic wastewater was fed through the bottom of the settled sludge bed with a superficial liquid velocity of $0.46 \,\mathrm{m}\,\mathrm{h}^{-1}$ (60 min). The remainder of the cycles were identical for both reactors: an aeration phase (maximum duration of 137 min), a settling period (minimum duration of 3 min), and finally the discharge of effluent (1 min) and a waiting phase to allow packing of the sludge bed (4 min). All sludge unable to meet the settleability criterion, was discharged with the effluent. During start-up, the settling period started at 30 min at the expense of the aeration phase and was gradually decreased to 5 min, while maintaining a constant total cycle duration. The temperature was controlled at 20 \pm 1 $^{\circ}$ C through the double-jacketed reactor wall using a water bath with thermostat. The pH was controlled during aeration (and during the mixed anaerobic phase of the pulse-fed reactor) at 7.0 \pm 0.1 by dosage of either a 1 M solution of hydrochloric acid or a 1 M sodium hydroxide solution. A conductivity sensor was used to monitor the anaerobic release and aerobic removal of ortho-phosphate (Weissbrodt et al., 2014). During aeration, a recirculation gas flow was maintained at 6 L min-1 (superficial gas velocity of 4.2 cm s⁻¹). A dissolved oxygen (DO) concentration of 2 mg L^{-1} was maintained during the aeration phase via addition of compressed air or dinitrogen gas using mass flow controllers. The total organic loading rate $(1.12 \text{ g COD L}^{-1} \text{ d}^{-1})$ was kept constant over the course of the study. Granular sludge previously enriched under the same conditions as applied in the bottom-fed reactor, and with the same synthetic influent, was used as inoculum. The inoculum was crushed using an ULTRA-TURRAX homogenizer T-18 (IKA, Staufen im Breisgau, Germany), after which the sieve fraction between 63 µm and 100 µm added to both reactors to yield an initial MLSS concentration of 0.5 g L⁻¹.

2.2. Composition of synthetic wastewater

A synthetic wastewater of 1.4 L per cycle was used as anaerobic feed and consisted of 1.2 L of deionized water together with 100 mL carbon source (medium A) and 100 mL nitrogen and phosphorous source (medium B). Medium A contained 65.6 mM NaCH₃COO·3H₂O, 4.1 mM MgSO₄·7H₂O, and 5.4 mM KCl. Medium B contained 15 mM NH₄Cl, 1.3 mM K₂HPO₄, 2.1 mM KH₂PO₄, and 16.6 mL L⁻¹ trace elements solution (Vishniac and Santer, 1957), but using 2.2 mg L⁻¹ ZnSO₄·7H₂O instead of 22 mg L⁻¹ (Pronk et al., 2015). The combination of medium A, medium B, and tap water led to a synthetic wastewater composition of 300 mg COD L⁻¹, 15 mg NH₄⁺-N L⁻¹, and 7.5 mg PO₄³-P L⁻¹. Allylthiourea (ATU, 5 mg L⁻¹ synthetic wastewater) was dosed to suppress nitrification. This enabled the calculation of biomass yield directly from the consumption of ammonium and ensured anaerobic conditions at the start of the feeding phase due to the absence of nitrate from the previous

cycle. All media were dosed using peristaltic pumps.

2.3. Batch test for determination of anaerobic kinetics and acetate storage capacity

Anaerobic batch tests were performed on the granule size fractions obtained by sieving once a dynamic equilibrium had been reached in the granule size distribution in both reactors (after 140 days). A mixed sludge sample was obtained at the end of the aeration phase and fractionated over a stack of sieves with varying mesh size (fractions 400-800 μm , 800-1000 μm , 1000-1400 μm and >1400 μm). Each fraction was added to a separate container with filtered reactor effluent (63 μ m) to obtain a total volume of 200 mL, containing 0.1 M HEPES acting as a buffer to ensure a constant pH throughout the experiment, equivalent to normal reactor operation. The pH was set to 7 \pm 0.5 using a 4 M solution of sodium hydroxide. Temperature was constant throughout the experiment at 20 °C. Each container was sparged with dinitrogen gas (1 L min⁻¹) for 5 min to strip dissolved oxygen from the liquid, after which a sample was taken for the initial ortho-phosphate concentration. Sparging continued throughout the remainder of the experiment to maintain anaerobic conditions. The experiment was initiated by addition of a concentrated solution of sodium acetate to obtain an initial concentration of 500 mg Ac- L^{-1} to prevent incomplete penetration of the largest granule size (full penetration up to largest granule size of 1.5 mm and t₉₀ penetration time of 5.3 min according to Stewart (2003) using $D = 0.87 \cdot 10^{-9} \text{ m}^2 \text{ s}^{-1}$ (van den Berg et al., 2021b) and $q_{Ac,max} = 0.15 \text{ g Ac}^- \text{ g VSS}^{-1} \text{ h}^{-1}$ (this work)). After addition of the sodium acetate, a sample (approximately 2.5 mL) was taken every 5 min (up to 30 min) and immediately filtered through a 0.45 μm syringe filter (CA membrane, Millipore) and put on ice for later determination of ortho-phosphate and acetate concentration profiles. A final sample was taken after 100 min to determine total release of ortho-phosphate and uptake of acetate. Negligible biomass was removed during sampling. The decrease in liquid volume due to sampling was determined after the experiment had finished, which was used in the calculation of the specific activity of the biomass. The biomass in each container was sampled for determination of the MLVSS concentration after the experiment had finished.

2.4. Analytical procedures

2.4.1. Determination of ML(VSS), solute concentrations and sludge volume (index)

NH $_{+}^{+}$ -N and PO $_{+}^{3}$ -P concentrations were measured by using a Thermo Fisher Gallery Discrete analyser (Thermo Fisher Scientific, Waltham, USA). The concentration of acetate was determined by high-performance liquid chromatography (HPLC) with an Aminex HPX-87H column from Biorad, coupled to an UV detector, using 0.01 M phosphoric acid as eluent. Mixed liquor suspended solids (MLSS) and volatile suspended solids (MLVSS) concentrations in the reactor were determined according to the standard methods ("2540 SOLIDS," 2017). The sludge volume after 5 min of settling (SV $_{5}$) was determined in-situ in between cycles.

2.4.2. Biomass density within granules

The biomass density of the granules was measured using a Dextran Blue-method (Beun et al., 2002; van den Berg et al., 2021a). A dilution series of Dextran Blue 2000 was prepared in the filtered effluent (0.45 μm CA membrane, Millipore) up to 2 g L $^{-1}$ and the absorption of light at a wavelength 620 nm measured with a spectrophotometer (DR3900, HACH) as a calibration line. The whole sludge volume from a reactor was transferred to a measuring cylinder and effluent was added to a total volume of 1 L. Effluent collected from the previous cycle was decanted and filtered through a 0.45 μm filter. 1 g of Dextran Blue 2000 was added to the measuring cylinder and subsequently the whole cylinder was mixed. The total volume and settled sludge volume were measured after

five min of settling. Samples were in taken from the supernatant in triplicate and filtered through a $0.45~\mu m$. After determination of the concentration of Dextran Blue 2000 by spectrophotometry, the volume occupied by the biomass was calculated and combined with the VSS previously determined to yield the biomass density.

2.4.3. Level of PHAs in granule sieve fractions before and after anaerobic feeding

Mixed biomass samples were taken after the anaerobic reaction phase and at the end of the aeration phase of both reactors to determine the average acetate stored as PHAs per granule sieve fraction. The bottom-fed reactor was modified to accommodate anaerobic sampling after the feeding. During the feeding, the liquid above the sludge bed was stripped with nitrogen gas to remove residual oxygen without disturbing the influent flow through the bed. After anaerobic feeding, the bottom-fed reactor was mixed by sparging dinitrogen gas and a mixed biomass sample was taken. The biomass was inactivated with formal-dehyde and subsequently sieved (fractions <400 μ m, 400–800 μ m, 800–1000 μ m, 1000–1400 μ m and >1400 μ m) to prepare for determination of the P3HB and P3HV content of each size fraction according to the method of Johnson et al. (Johnson et al., 2009).

2.4.4. Stereozoom microscopy for counting individual granules

Sludge was collected from the reactor at the end of the aeration phase and from the effluent directly after discharge while kept in suspension. A mixed sample from either source was transferred to a glass petri dish and examined according to Gjaltema et al. (1995) by the means of an Olympus reverse microscope coupled with a Leica Digital Camera, together with its software QWin Pro (version 3.1.). The granule size distribution was determined by counting individual granules with a minimum of 1000 hits. The equivalent diameter of each granule was calculated based on the projected area of a granule, which was used to calculate the volume assuming the shape of a sphere. False hits were identified by manual inspection of a subset of the images obtained in one measurement. These false hits were consistently caused by aberrations in the glass dish containing the sample and were smaller than 100 μm . Therefore, hits with an equivalent diameter smaller than 100 μm were discarded.

2.4.5. Fluorescent in-situ hybridization (FISH)

The handling, fixation and staining of FISH samples was performed as described by Bassin et al. (2011). A mixture of PAO462, PAO651, and PAO846 probes (PAOmix) was used for visualizing polyphosphate accumulating organisms (PAO) (Crocetti et al., 2000). A mixture of GAOQ431 and GAOQ989 probes (GAOmix) was used for visualizing glycogen accumulating organisms (GAO) (Crocetti et al., 2002). A mixture of EUB338, EUB338-II and EUB338-III probes was used for staining all bacteria (Amann et al., 1990; Daims et al., 1999). Images were taken with a Zeiss Axioplan 2 epifluorescence microscope equipped with filter set 26 (bp 575e625/FT645/bp 660e710), 20 (bp 546/12/FT560/bp 575e640) and 17 (bp 485/20/FT 510/bp 5515e565) for Cy5, Cy3 and fluos respectively.

2.5. Calculation procedures

2.5.1. Granule size distribution

Hits from counting individual granules through stereozoom microscopy were binned in size fractions $<\!400~\mu m,\,400–\!800~\mu m,\,800–1000~\mu m,\,1000–1400~\mu m$ and $>\!1400~\mu m$ based on the equivalent diameter. A volume was calculated for each granule in every bin by assuming sphericity. Finally, the mass distribution over each bin was calculated by multiplying the volume fraction of a bin of the total volume of all counted granules, assuming a constant biomass density not dependant on granule size.

2.5.2. Conversion of PHA mass fractions to acetate equivalents

A ratio of 0.75 C-mol acetate/C-mol P3HB was used to calculate the anaerobically consumed acetate equivalents for the measured P3HB for both PAM and GAM (Smolders et al., 1995b; Zeng et al., 2003). Besides P3HB, the accumulation of P3HV in acetate fed communities dominated by PAO occurs in the case of low phosphate availability (Silva et al., 2020; Welles et al., 2017). The energy required for the sequestration of acetate is then derived partly from glycolysis besides the hydrolysis of poly-phosphate. The surplus reduction equivalents from glycolysis are used to reduce either part of the acetyl-CoA (glyoxylate shunt) or of the glycolysis products (reductive branch of the tri carboxylic acid (TCA) cycle). Both yield propionyl-CoA, which is subsequently converted with P3HB to P3HV (and to small amounts of PH2MV, disregarded in this analysis). Based on the conditions applied, it was assumed that all P3HV originated from pure GAM metabolism, yielding a ratio of acetate carbon incorporated in P3HV of 0.26 C-mol/C-mol (Zeng et al., 2003).

2.5.3. Calculation of anaerobic acetate distribution

The anaerobic acetate distribution over the sludge population was calculated by combining the granule size distribution (f_i), total sludge volume (V_s) biomass density ($\rho_{X,VSS}$) and acetate equivalents calculated from the difference of PHA levels at the end of the aerated phase and the end of the anaerobic phase (ΔAc_i^-). The procedure for the fraction of acetate fed (Ac_{fed}^-) in a size fraction (f_{i,Ac}-) is depicted in Eq. (1):

$$f_{i,Ac^{-}} = f_{i}V_{S}\rho_{X,VSS}\frac{\Delta Ac_{i}^{-}}{Ac_{fod}^{-}}$$
 (1)

2.5.4. Determination of SRT of granule size fractions

The SRT for the granule size fractions at steady-state were calculated based on the cumulative excess sludge removed during one day via selective wasting and the granule size distribution in the reactor. The collected excess sludge was fractioned via a stack of sieves with mesh sizes $1400~\mu m$, $1000~\mu m$, $800~\mu m$ and $400~\mu m$ and the amounts TSS were subsequently determined for all fractions (WSi, g TSS d $^{-1}$). The fraction smaller than $400~\mu m$ was negligible at steady state and was therefore discarded. The total mass of sludge of each fraction was calculated from the granule size distribution and MLSS concentration in the reactor (Si). The SRT of a size fraction (SRTi, day) was calculated from through the Eq. (2):

$$SRT_{i} = \frac{WS_{i}}{S_{i}}$$
 (2)

3. Results

3.1. Start-up

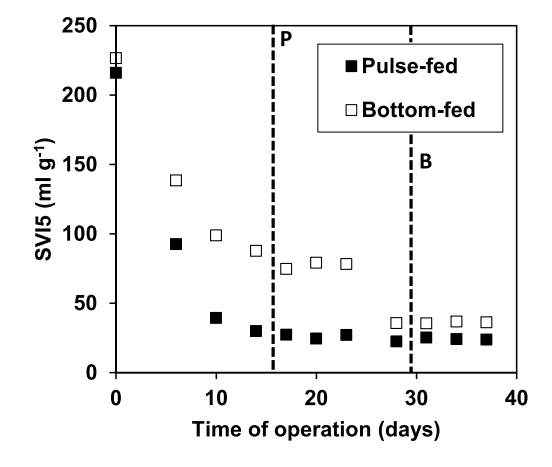
The pulse-fed and bottom-fed reactors were both inoculated with approximately 0.5 g TSS L^{-1} of crushed aerobic granular sludge previously enriched in a laboratory reactor operated under similar conditions (Haaksman et al., 2020). The crushed seed sludge was sieved over a cascade of a 100 μm and a 63 μm sieve, after which the fraction retained at the 63 μm sieve was used as inoculum (Fig. 1). Both the reactors were immediately operated under the same volumetric substrate (acetate) loading rate of 1.12 g COD L^{-1} d $^{-1}$. The initial settling rate selection criterion was set at 1 m h^{-1} and was gradually increased to 10 m h^{-1} over the course of 19 days for both reactors.

3.1.1. Settleability and morphology

Development of the granular sludge in terms of SVI₅ and MLSS in the reactors is depicted in Fig. 1. Both reactors developed well settling granular sludge (SVI₅ between 30 and 40 ml g⁻¹), but the granulation occurred faster in the bottom-fed reactor (26 μm d⁻¹ for the pulse-fed reactor, versus 40 µm d⁻¹ for the bottom-fed reactor). The amount of dry mass increased at a similar rate, regardless of the anaerobic feeding regime. The initial growth morphology of both systems was characterized by flocculent as well as granular growth (Fig. 1A, B). Flocs were identified as translucent clusters using stereo zoom microscopy, while small granules (100-200 µm) appeared as non-translucent and dense aggregates. Flocculent growth could not be detected in the pulse-fed reactor after 15 days (Fig. 2C), while flocs were observed in the bottom-fed reactor up to 28 days of operation. These observations coincided with the development of the sludge volume index (SVI₅, Fig. 1A). The further development of the granular morphology was similar for both anaerobic feeding regimes.

3.1.2. Anaerobic acetate uptake efficiency

The anaerobic acetate uptake was monitored on-line by conductivity measurements (see figure S1 for the estimated completeness of acetate uptake as function of time). The pulse-fed system developed complete anaerobic acetate uptake within two weeks after start-up. The bottom-fed reactor took four weeks for obtaining full anaerobic acetate uptake. This was due to short-cut flow of the influent through the sludge bed during the first month after start-up, decreasing the effective anaerobic contact time with the sludge. Therefore, part of the fed acetate was then not taken up anaerobically. This can be considered a scale-effect due to the limited sludge bed height and less optimized influent distribution manifold compared to full-scale reactors. This prolonged the aerobic availability of acetate compared to the pulse-fed reactor and



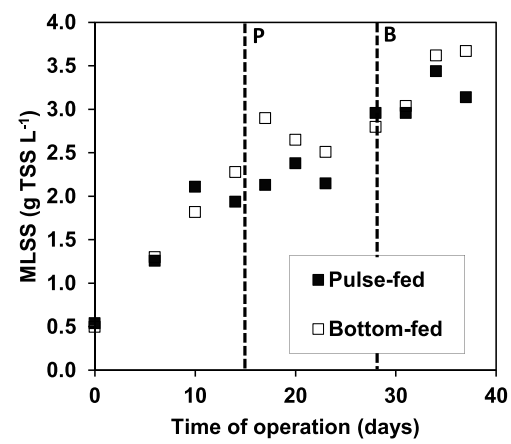


Fig. 1. Development of SVI_5 (left) and MLSS (right) over time for the pulse-fed (solid squares) and bottom-fed (open squares) reactors. Vertical dashed lines denote transition to only granular growth as observed using stereozoom microscopy for both the pulse-fed (P) and bottom-fed (B) reactors.

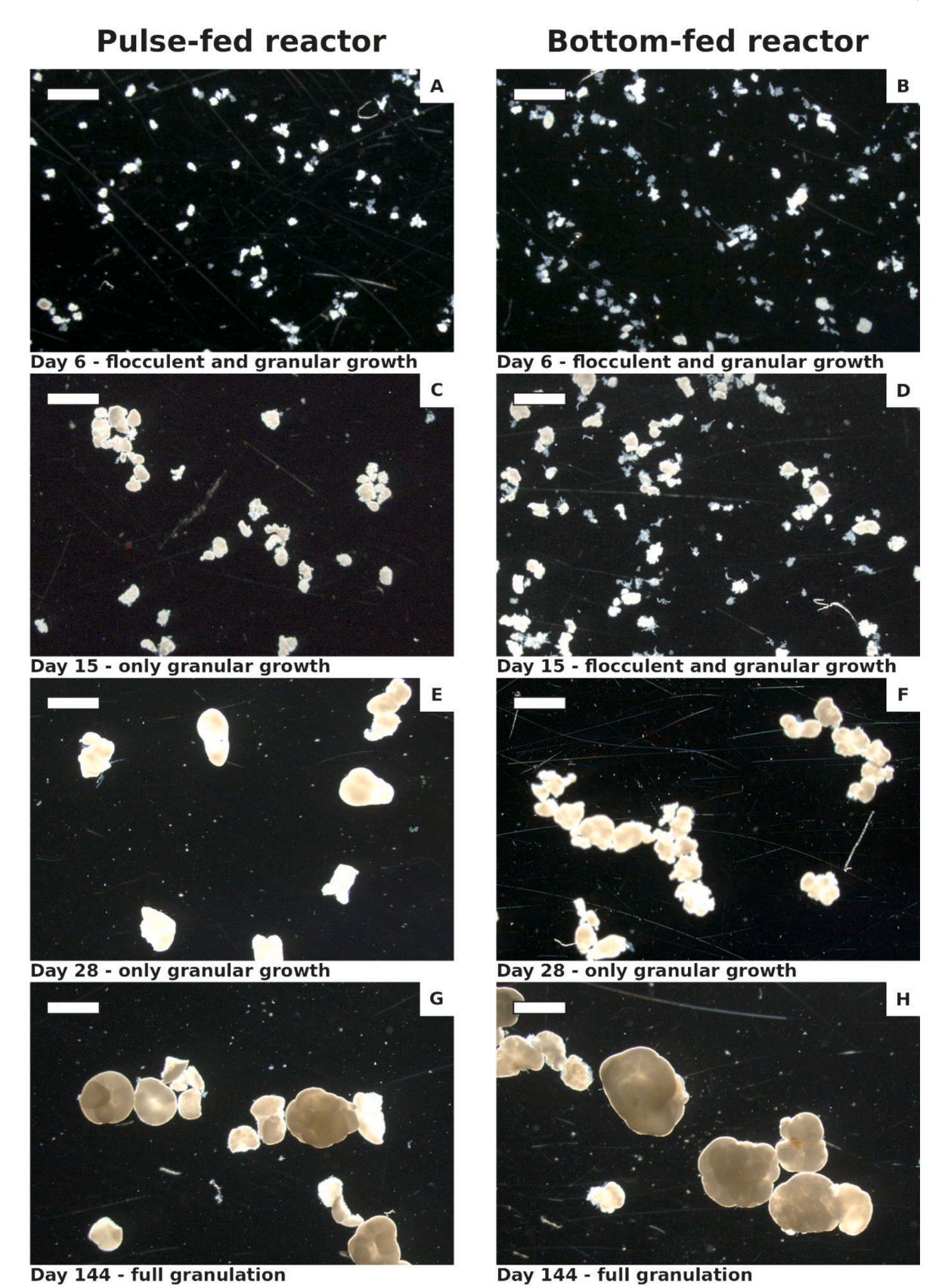


Fig. 2. Development of sludge morphology as observed by stereo zoom microscopy. Four stages in the development are depicted for both the pulse-fed and bottom-fed reactors: 6 days after start-up (A + B), 15 days after start-up (C + D, complete granular growth in pulse-fed reactor), 28 days after start-up (E + F, complete granular growth in bottom-fed reactor) and 144 days after start-up (E + F). Scale bar represents 1000 μm.

caused the extended presence of flocs in the bottom-fed reactor. The disappearance of flocculent growth coincided in both reactors with the moment of full anaerobic acetate uptake in the pulse-fed and bottom-fed reactors at days 15 and 28, respectively.

3.2. Steady-state operation

The pulse-fed and bottom-fed reactors were operated for a duration of 5 months until a stable granule size distribution had been achieved. Both systems were characterized and typical process parameters for both reactors are listed in Table 1. The reactors have been operated at a similar average MLVSS concentration, substrate loading rate and SRT. Considering the fluctuations in MLVSS concentration (sampled over the course of five weeks, centred around 144th day of operation), the biomass characteristics had developed to a similar level in both reactors. The bottom-fed reactor showed a slightly higher SVI, which had been observed since the start of the experiment. Other than that, the difference in anaerobic feeding regime did not result in differences in biomass characteristics. FISH microscopy indicated an enrichment of Ca. Accumulibacter phosphatis clade I at similar high levels in both reactors (Figure S3). The mass distribution over the granules size fractions showed a higher unevenness for the bottom-fed reactor compared to the pulse-fed reactor; 81% of the mass was present in granules larger than 1 mm in the bottom-fed reactor, compared to 66% in the pulse-fed reactor (Fig. 3). The main difference in biological nutrient removal was the substantially higher anaerobic P/COD-ratio and higher aerobic specific phosphate uptake rate of the pulse-fed reactor. Other reactor characteristics relevant for further analysis of the effect of the anaerobic feeding regime on aerobic granulation are reported below.

3.3. PHA storage polymer distribution over granule size fractions

The impact of the anaerobic feeding regime on the distribution of acetate over the granule size fractions was assessed once the granule population had stabilized in both the pulse-fed and bottom-fed reactors. Samples were taken from the mixed granular sludge suspension before and after the anaerobic feeding stage within the same cycle. The mass

Table 1Overview of biomass characteristics (based on data from five consecutive weeks) and parameters regarding biological conversions.

| Property (unit) | Pulse-fed | Bottom-fed |
|--|--|--|
| MLVSS (g VSS L^{-1} reactor) Organics content (g VSS g^{-1} TSS) Sludge volume (mL bed L^{-1} reactor) Sludge volume index (mL bed g^{-1} TSS) Biomass density (g VSS L^{-1} biomass) ^a Estimated biomass yield (g VSS g^{-1} COD) ^d Average SRT based on yield (d) ^d | 3.7 ± 0.7 0.79 ± 0.03 149 ± 19 33 ± 1 31 0.19 18 | 3.5 ± 0.6 0.82 ± 0.03 184 ± 34 39 ± 2 27 0.19 18 |
| Anaerobic conversions | | |
| P/COD-ratio (g g ⁻¹) ^b max. Ac ⁻ uptake rate (mg COD g ⁻¹ VSS h ⁻¹) ^c max. Ac ⁻ uptake capacity (mg COD g ⁻¹ VSS) ^c | 0.57 156 155 | 0.32 149 145 |
| Aerobic conversions | | |
| PO ₄ -P uptake rate (mg g $^{-1}$ VSS h $^{-1}$) ^b Initial NH ₄ —N uptake rate (mg g $^{-1}$ VSS h $^{-1}$) ^b NH4-N/VSS (g g $^{-1}$) ^d | 34 0.67 0.11 | 18 0.44 0.11 |

a) Determined using Dextran Blue-method.

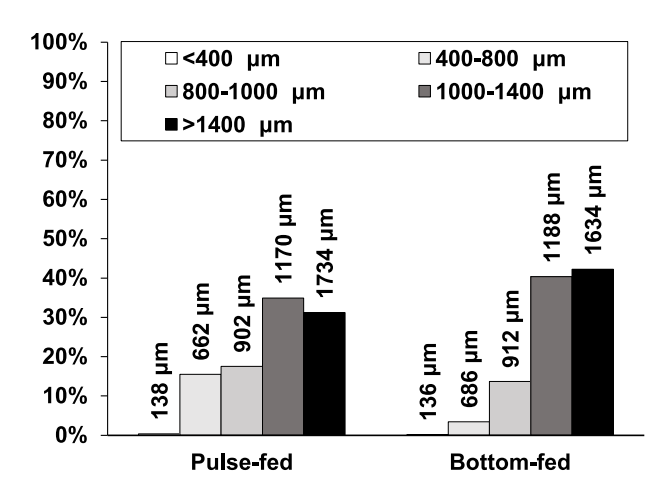


Fig. 3. Mass distribution (VSS) over granule size fractions in both the pulse-fed and bottom-fed reactors based on stereo zoom microscopy and bed porosity measurements. Labels represent the mean particle size per fraction as determined via analysis of images obtained using stereozoom microscopy. Sludge samples were taken at steady state conditions on day 144 of operation.

fractions of P3HB and P3HV in the sludge samples were quantified after fractionation by sieving. The majority of the PHA storage pool was P3HB, but considerable amounts of P3HV were detected in both the pulse-fed and bottom-fed systems (Table S1). The levels of PHB and PHV in the biomass were converted to the equivalent amount of acetate consumed before and after the anaerobic phase per amount of VSS (Fig. 4). A decreasing trend was observed for the relative amount of acetate consumed in the pulse-fed system for increasing granule size fraction. On the other hand, the anaerobic bottom-feeding favoured substrate uptake by the largest granule size fraction. A considerable amount of PHA remained in the bottom-fed reactor at the end of aeration, and this amount increased with granule size. The pulse-fed system showed a complete depletion of the PHA storage pool. Negligible differences were observed between anaerobic acetate uptake rates and maximal storage capacities between both reactors and per sieve fraction in batch tests (Table 1). Therefore, the observed differences can be attributed to the difference in anaerobic contact mode applied in each reactor.

3.4. Anaerobic acetate load distribution and solids residence time

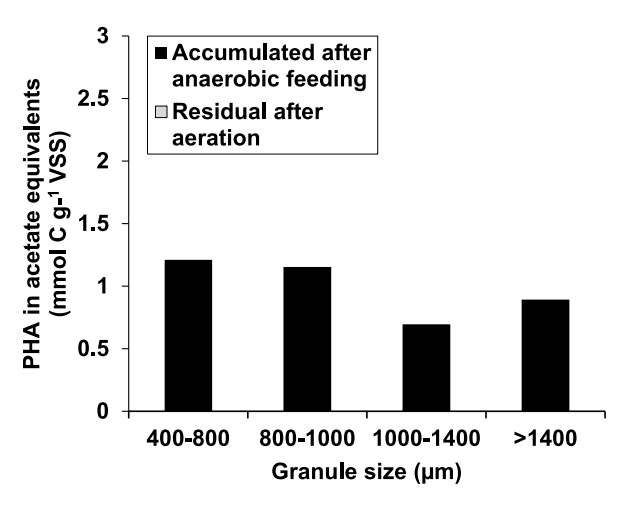
To show the acetate load difference between the anaerobic feeding regimes, the amounts of acetate converted to PHA were combined with the measured VSS distributions over the granule size fractions in each reactor (Fig. 5). Using this approach, 94% and 81% of the acetate loads per cycle were recovered for the pulse-fed and bottom-fed reactors, respectively. In the bottom-fed reactor a negligible expansion of the settled sludge bed was observed during the anaerobic phase and no acetate could be detected in the bulk-liquid above the sludge bed throughout the anaerobic phase. The acetate concentration in the bulkliquid therefore decreased from the initial level in the synthetic wastewater at the inlet to depletion before exiting at the top of the sludge bed. Although both reactors had fully granulated with similar size distributions, the net acetate distribution differed substantially. The pulse-fed system showed minor differences in acetate load distribution over the granule size fractions, while most of the acetate load was anaerobically consumed by the largest granule size fractions (>1 mm) present in the bottom-fed reactor.

The acetate load distribution data were subsequently used to calculate the sludge loading rate per size fraction in both reactors. The mass distribution over the granule size fractions in the reactor, sludge wasted selectively with the effluent and sludge wasted manually were then used to calculate the SRT of the individual granule size fractions. The granule

b) Calculated based on cycle measurement(s) (see Figure S2).

c) Maximum acetate uptake rates and storage capacity under anaerobic conditions were determined in batch tests with a surplus of substrate for each reactor and for each sieve fraction. Negligible differences were observed between sieve fractions, therefore average values were reported per reactor.

d) The synthetic wastewater was supplemented with allylthiourea to inhibit nitrification. The reported ratios of aerobically consumed NH4-N/fed COD were therefore directly related to biomass formation.



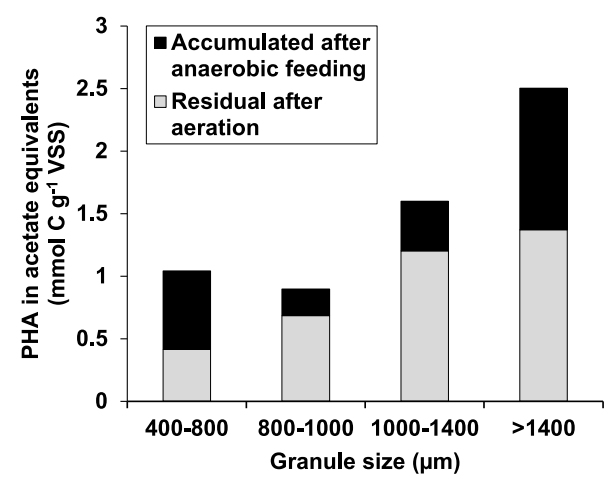


Fig. 4. PHA storage polymer contents per granule size fractions expressed as acetate equivalents consumed during the anaerobic feeding phase (cumulative P3HB and P3HV) for the pulse-fed reactor (left) and the bottom-fed reactor (right). Sludge samples were taken at day 144 of operation.

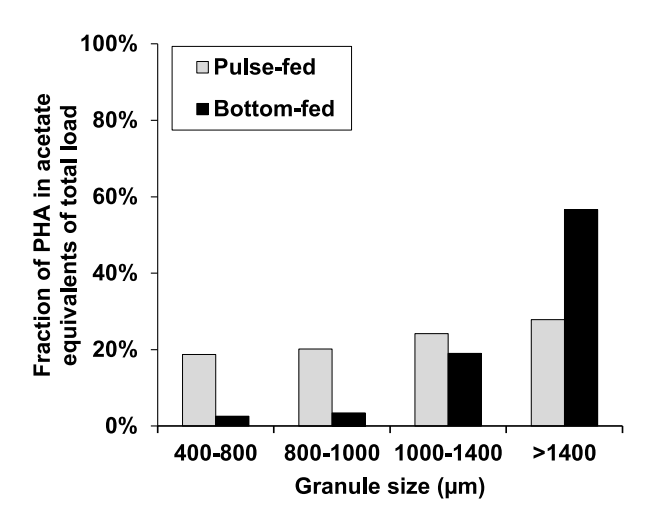
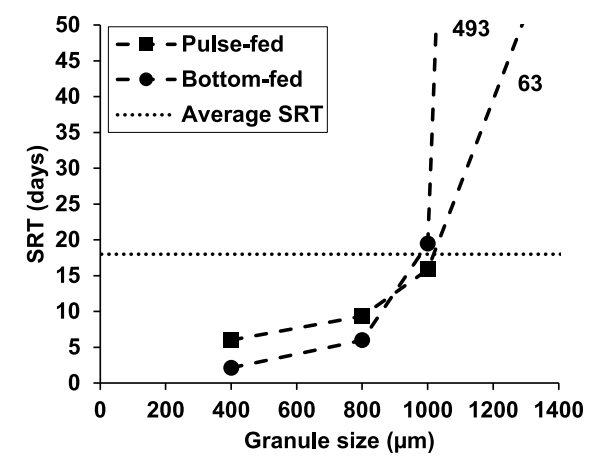


Fig. 5. Anaerobic acetate load distribution over the granule size fractions for the pulse-fed and bottom-fed reactors. Distribution was calculated based on consumed acetate equivalents of difference in PHA content before and after anaerobic feeding. Samples were taken at day 144 of operation.

size distribution of all sludge removed from the reactor was averaged over a period of five days in the same week as the samples for measurement of the PHA content had been taken. Both the sludge loading rate and SRT per granule size fraction are depicted in Fig. 6. Both systems showed an increase in SRT for an increasing granule size, regardless of the anaerobic feeding strategy. The SRT of the fraction $>\!1400\,\mu m$ was shorter in the pulse-fed reactor than in the bottom-fed reactor due to unintended accumulation of large granules in the effluent discharge port during aeration. This had only a minor effect on the obtained size distribution compared to the bottom-fed reactor. In the pulse-fed reactor the loading rate decreased as the granule size increased. For the bottom-fed reactor, the sludge loading rate increased with increasing granule size.

4. Discussion

Two sequencing batch aerobic granular sludge reactors were operated to investigate the effect of the anaerobic contact mode on acetate distribution over granular size fractions and its effect on sludge granulation and dynamics of EBPR organisms. Synthetic wastewater was anaerobically pulse-fed in one reactor, while bottom-feeding was applied in the other. Both reactors were inoculated with the same crushed aerobic granular sludge and were operated in the same way except for the aforementioned anaerobic phase. The observed differences in the steady-state characterization will be discussed next in more



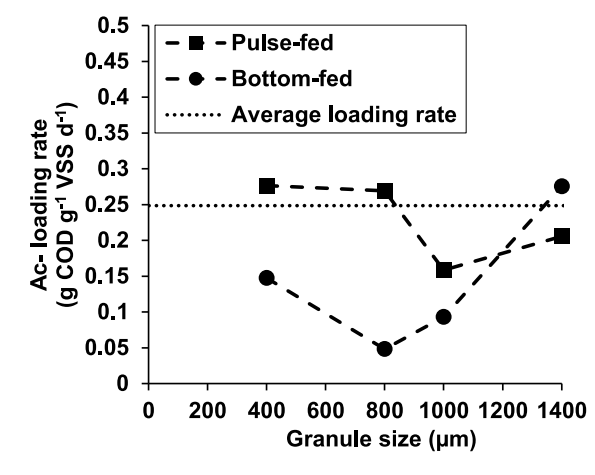


Fig. 6. Comparison between solids retention time (left) and acetate sludge loading rate (right) of granule size fractions between the pulse-fed (dashed line, closed squares) and bottom-fed (dashed line, closed circles) reactors. Reactor averages were the same in both systems for acetate loading rate and solids retention time, denoted by dashed horizontal lines.

detail in relation to the applied anaerobic contact mode.

4.1. Acetate distribution over granule size fractions

The biomass specific anaerobic acetate uptake (mmol C Ac⁻equivalents g⁻¹ VSS) and storage as PHA was nearly independent of granule size for the pulse-fed reactor, while for the bottom-fed reactor there was a clear increasing acetate uptake with increasing granule size (Fig. 6). Experimental estimation of the maximum acetate storage capacity (150 mg $Ac^ g^{-1}$ VSS), specific anaerobic acetate uptake rate (150 mg $Ac^ g^{-1}$ VSS h^{-1}) and biomass concentration were similar for both reactors (Table 1). Also, the dominant PAO clade, determined by FISH, was the same in both reactors (clade I). This indicates that the potential of the microbial EBPR population was highly similar between both operating regimes, and in both systems the maximum acetate uptake capacity was not limiting the observed acetate uptake (granules close to the influent distributor in the bottom-fed reactor could only just be saturated at the end of the 60-minute feeding period). This indicates that the differences in COD loading can be explained by the differences in liquid-biofilm mass transfer to the granules for the two anaerobic feeding modes. The driving force from the concentration of acetate in the bulk liquid over time and place experienced by granules, and mass transfer rate are the main differentiating variables.

For the pulse-fed reactor, both the acetate concentration and effective contact time were the same for all granules due to the mixed anaerobic reaction phase. Therefore, the liquid-biofilm mass transfer was the determining mechanism. The mass transfer coefficient through a liquid-biofilm interface depends on liquid velocity local around the biofilm and the surface area. Since the surface to volume ratio decreases with increasing granule size, the overall mass transfer coefficient decreases for increasing granule size (Cussler, 2009; Nicolella et al., 1998). Effectively, the efficiency of the granular volume usage decreases with increasing granule size (Liu et al., 2005). The extent of the actual difference in loading between, depends on the initial penetrated volume. The near equal acetate loading with a slightly decreasing trend with increasing granule size observed in the pulse-fed reactor is consistent

with substrate uptake limited by surface-to-volume ratio. The effect is limited due to the high initial acetate concentration, acetate loading rate and selective retention of larger granules. If an anaerobic zone with mixed tanks-in-series would get continuous feeding with real wastewater, as in a continuous flow system with both lower concentrations of rbCOD and rbCOD loading rate, the advantage for smaller granules would be more pronounced.

The same analysis yields a different result for the bottom-fed reactor. The observed increase in anaerobic acetate loading with increasing granule size is due to a decreasing acetate concentration together with a (potentially) decreasing average granule size over the height of the sludge bed. The mass transfer limitation for granules of increasing size, due to the decreasing surface to volume ratio, is thus counteracted and reversed by the higher probability for larger granules to experience a higher bulk-liquid substrate concentration. The importance of this selective feeding of the largest granule size fraction has recently been underlined as one of the main mechanisms for stable aerobic granulation in bottom-fed AGS reactors in practice (van Dijk et al., 2022). Bottom-feeding through a sludge bed thus favours increased anaerobic substrate uptake by the larger granule size fractions. The difference in the distribution of stored substrate forced by the anaerobic contact mode is illustrated in Fig. 7.

4.2. COD loading rate versus SRT

Both the pulse-fed and bottom-fed reactors showed an increasing SRT for increasing granule size fractions (Fig. 6A). Such a trend was expected based on the preferential wasting of slower settling sludge fraction as means of granular sludge selection. For the COD loading rate on the other hand (Fig. 6B), the pulse-fed system showed a slight decrease with granule size, while in the bottom-fed reactor the acetate loading rate increased substantially with granule size. In continuous flow-through CAS-systems, the sludge loading rate decreases on average with increasing SRT for all sludge particles (Metcalf and Eddy, 2013). This relation does also apply to AGS systems on average. In CAS-systems, however, the probability distributions around the average of both

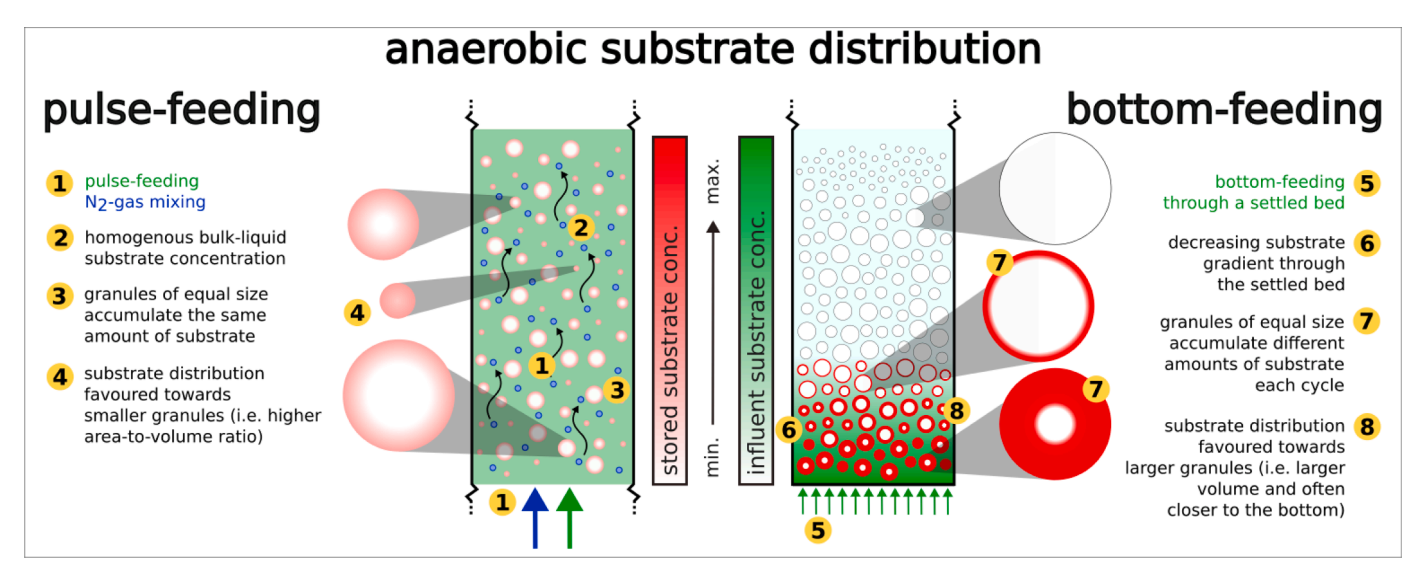


Fig. 7. Schematic representation of the difference in the anaerobic distribution of stored substrate forced by the anaerobic contact mode (either pulse-feeding (left) or bottom-feeding (right)). A random part of the pulse-feed bubble column is depicted, while the settled sludge bed is shown for the bottom-feed reactor. The shading of the bulk-liquid depicts the maximum substrate concentration during the anaerobic feeding of influent (pulse-feeding: 2 min, bottom-feeding: 60 min) as a fraction of the substrate concentration in the influent. The maximum bulk-liquid concentration of substrate in turn determines the maximum penetration depth achieved during the total anaerobic reaction time 60 min for both reactors. The radial colour gradient in the granules of represents the local concentration of stored substrate inside a granule after feeding. Influent concentration of substrate (acetate): 0.3 g COD L⁻¹. Maximum concentration of stored substrate inside a granule (acetate-equivalents): 4.5 g COD L⁻¹. Blue circles and black arrows depict the mixing through sparging of dinitrogen gas during and after pulse-feeding. Legend of numbers: (1, 5): anaerobic feeding mode, (2,6): resulting bulk-liquid substrate concentration pattern, (3, 6): difference in substrate accumulation for equally sized granules per cycle, (4, 8): trend of overall substrate distribution due to anaerobic feeding mode.

substrate and sludge discharge follow the hydraulic residence time distribution, without any impact of the properties of sludge particles (e. g. size or difference in settling rate). In this study, the average sludge yield was the same for both reactors, however the difference between granules sizes indicates that the internal redistribution of biomass growth between size fractions was different in the pulse-fed reactor compared to the bottom-fed reactor. The redistribution of biomass from larger to smaller aggregates is a common property of biofilm systems, which balances growth and biomass removal (Pereboom, 1994). This yields an increase of SRT deeper into a biofilm (Tijhuis et al., 1994), and is specifically of interest for aerobic granular sludge systems performing EBPR (Morgenroth and Wilderer, 1999; Winkler et al., 2012). While the SRT distribution of biofilm aggregates of different sizes can be influenced via selective wasting and process conditions affecting detachment, adjusting the distribution of substrate (i.e. the distribution of biomass growth) over size fractions is more difficult. The kinetics of substrate uptake and mass transfer determine the distribution of growth in biofilm systems with completely mixed reactors, as was previously discussed for the pulse-fed reactor. The comparison with a bottom-fed reactor in the current study shows that the uncoupling of COD uptake in the anaerobic phase from growth in the aerobic phase in aerobic granular sludge systems provides a means of control over the distribution of biomass growth.

This has two main implications. First, the granule size distribution can be influenced by directing the available COD towards smaller or larger granules. Second, the anaerobic penetration depth of COD can be influenced, which in turn influences the location of microbial conversions within granules. The anaerobic contact mode thus provides an additional tool that can be used to optimize the granule size distribution and biological nutrient removal in aerobic granular sludge processes for wastewater treatment.

4.3. Residual levels of PHA after aeration

A remarkable difference in residual PHA levels at the end of aeration was observed between the pulse-fed and bottom-fed reactors. The bottom-fed reactor showed substantial levels of residual PHA after aeration for all granule size fractions, while the fractions were depleted of PHA in the pulse-fed reactor (Fig. 4). Cultures enriched for EBPR have been shown to exhibit flexibility in the residual PHA content depending on the operational parameters, including SRT (Smolders et al., 1995a), influent P/COD-ratio (Welles et al., 2017), polyphosphate storage levels (Acevedo et al., 2012), pH (Filipe et al., 2001a), and cycle length (Kuba et al., 1997). The operational conditions during the aerobic phase were the same for both reactors (i.e. k_La, dissolved oxygen concentration and duration) and thus did not cause the difference in remaining PHA. The remaining PHA was observed in all granule size classes of the bottom fed reactor, indicating the residual levels of PHA were not affected by the differences between the granule size distributions of the reactors. Therefore, the anaerobic contact mode likely caused this difference, specifically the ratio of anaerobic loading of acetate of a granule size fraction to aerobic time.

In completely mixed enrichment cultures and in the pulse-fed granular system presented here, most organisms in the active layer of all granular size fractions experience the same conditions each cycle, i.e. same amount of acetate taken-up, same penetration depth and same aerobic time to convert it. This gives the organisms the opportunity to fully optimise their resource allocation to maximal growth (Silva et al., 2019). In the bottom-fed reactor, all granules are distributed over the settled bed prior to the anaerobic feeding. The largest granules will be more distributed towards the bottom of the sludge bed while the smallest granules would be more towards the top. It was estimated that the acetate front reached up to 36% of the sludge bed from the bottom of the reactor, based on the measured specific acetate uptake rate, bed porosity and superficial liquid velocity during feeding (Figure S4). The partial anaerobic contact of the sludge bed with acetate led to a highly

variable acetate uptake for a granule per cycle, depending on its position in the sludge bed after settling. Although larger granules have a higher probability of settling more towards the bottom of the sludge bed, the applied superficial liquid velocity during feeding (i.e. $0.46~\mathrm{m~h^{-1}}$) is well below the minimum fluidization velocity. Therefore, negligible bed expansion and no further stratification were observed during feeding. Granules of all size fractions thus had a substantial probability of residing in the bottom part of the sludge bed and thus be in contact with acetate during feeding. This might force the organisms' storage metabolism into a more resilient state so it can deal with variations in substrate availability. This would underline the flexibility of $\it Ca.$ Accumulibacter phosphatis to modulate the metabolism for optimal carbon utilization to the prevailing conditions (Silva et al., 2020).

Another possible explanation is that the fixed length of the aerobic phase was too short to fully convert all PHA for that part of the granules that received a peak anaerobic loading during a specific cycle. Granules at the bottom of the bottom-fed reactor will have been exposed to acetate during the full 60 min of feeding and these granules will have therefore a higher PHA content than average. The aerobic time is equal for all granules, and potentially too short when a granules has been near the inlet at the bottom during feeding. This would, on average, lead to a residual level of PHA. This hypothesis could not be investigated any further based on the available data and could the topic of future study.

Some work has been done studying the effect of fluctuating operational conditions on the performance of EBPR (Schuler et al., 2011), mainly due to the residence time distribution in continuous flow-through reactors. However, the width of the anaerobic load distribution as observed in the bottom-fed reactor used here was substantially larger and cannot be directly compared. Furthermore, full-scale aerobic granular sludge systems will be even more variable than the lab scale systems. This effect has not been considered well in the literature, but is essential to further optimise EBPR systems, especially when employing AGS.

4.4. Impact of contact method on anaerobic storage metabolism

The anaerobic conversion stoichiometry of acetate to PHAs was, surprisingly, different for the pulse-fed and bottom-fed reactors as well as for different granule size fractions within each reactor; the ratio of P3HV/P3HB accumulated during the anaerobic phase was on average twofold higher in bottom-fed reactor compared to the pulse-fed reactor with the largest granule size fraction having the highest ratio (Table S1). Both reactors were dominated by Ca. Accumulibacter phosphatis (Figure S1). The observed amount of ortho-phosphate released anaerobically was lower in the bottom-fed reactor compared to the pulse-fed reactor. These two observations are congruent. The trend continued further during the aerobic phase, where a nearly two-fold lower specific aerobic phosphate uptake rate was observed in the bottom-fed reactor compared to the pulse-fed reactor (Table 1). It has been indicated before that Ca. Accumulibacter phosphatis has a flexible metabolism and can operate between a full phosphate accumulation metabolism (PAM) and a full glycogen accumulating metabolism (GAM) (Oyserman et al., 2016; Silva et al., 2020; Welles et al., 2015). It seems that the pulse-fed system operated at full PAM, while the bottom fed system exhibited a mixed PAM/GAM phenotype. FISH has confirmed a full absence of known GAOs in the microbial population, while Ca. Accumulibacter phosphatis clade I was dominant (Figure S3).

These observations underline again the ability of *Ca*. Accumulibacter phosphatis to modulate its metabolism depending on the environmental conditions (Silva et al., 2020), although the driver for the differences in metabolism were not determined. A decrease of the P/COD-ratio in the influent has been found to increase the ratio of GAM/PAM in suspended growth systems (Welles et al., 2017). In this study, this was likely not a factor since the influent composition was the same. Sufficient polyphosphate was present in both reactors at the applied average SRT for full PAM to take place. If the differences are examined at the aggregate

level (i.e. assuming similar microbial activity throughout each granule with negligible spatial gradients), the difference in PAM/GAM metabolism could be related to the aforementioned difference in PHA remaining at the end of the aeration phase. In that case, the PAM metabolism could be the most optimal metabolism for systems with stable substrate loading, while GAM metabolism contributes to resilience to more dynamic substrate loading per granule.

Another hypothesis is that differences in spatial gradients within granules contributed to the observed difference in PAM/GAM ratios between both reactors. The anaerobic penetration depth of acetate in the granules in the bottom-fed reactor is larger compared to granules in the pulse-fed reactor (Fig. 7). The aerobic penetration depth of oxygen was estimated to be similar for both reactors due to the same operational conditions (i.e. the same transfer resistances for gas-liquid and liquidbiofilms) during uptake of phosphate, and always more shallow than acetate. Oxygen only penetrates further into the granules once the phosphate in the bulk-liquid has been depleted, thereby limiting the interior of the granules to perform GAM. The outer regions initially penetrated with oxygen are able to perform full PAM. The spatial separation between metabolisms would be most pronounced for the granules in the bottom-fed reactor, which could in turn contribute the observed difference in PAM/GAM-ratio between anaerobic pulsefeeding and bottom-feeding at the reactor level.

These observations warrant further investigation into the effect on the metabolism of *Ca.* Accumulibacter phosphatis of both the dynamic anaerobic loading, as well as the effect of differences in penetration depth of acetate and oxygen on potential spatial separation of PAM and GAM within individual granules, which could not be separated in this study. If the impact of dynamic operational conditions is also reflected in the PAM/GAM ratio for *Ca.* Accumulibacter phosphatis, it might form a proxy for the study of the occurring variability on the cellular level.

4.5. Practical implications

The influent with acetate as sole carbon source combined with an anaerobic contact phase selects completely for granular growth morphology and low SVIs (Martins et al., 2004), regardless of the anaerobic contact mode applied. Municipal sewage contains lower concentrations of volatile fatty acids (Henze et al., 2000) than the synthetic wastewater used in this study. In full scale EBPR systems easy hydrolysable and fermentable COD, after biological conversion into VFA, also contribute to the growth of EBPR organisms (Brdjanovic et al., 2016, chap. 2.2: Enhanced Biological Phosphorus Removal; Drewnowski and Makinia, 2011; Tykesson et al., 2002). These extra microbial conversions will have to be considered when translating the observations here to full scale systems, however general principles can be deducted of the present work.

Design of the anaerobic feeding is an important aspect for obtaining stable aerobic granular sludge. The current implemented full-scale aerobic granular sludge process (Nereda® technology) applies bottom feeding and excess sludge extraction from the top of the bed. This removes the weakest settling part of the sludge and provides most substrate to the best settling (large granules) fraction of the sludge (van Dijk et al., 2022), thereby enhancing stability of the granular sludge bed. There are ongoing developments for alternative implementations of the AGS technology, in SBR as well as continuous systems. A completely mixed anaerobic feeding SBR has been proposed and tested at pilot scale (Rocktäschel et al., 2015). However, there it was shown that this only resulted in stable operation if the wastewater has already high acetate concentrations in the influent. With a large rbCOD fraction in the influent, like in this study, selective wasting based on sludge settleability becomes the main driver for stable granulation. This can be deduced from the similarity in the granule size distribution of both reactors with different anaerobic feeding modes. This underlines the observations in this study that granulation can be obtained independent of anaerobic feeding mode, but that bottom feeding more readily results in stable

operation if the influent composition is less favourable.

With the aim to further develop AGS technology in conventional continuous operated wastewater treatment systems (Kent et al., 2018), the attention for the design of the anaerobic contact tank is likely even more critical. As has been reported in existing plants with strong plug-flow conditions granule formation is already induced (Redmond et al., 2019; Wei et al., 2020), indicating the advantage of having a strong concentration gradient as in the pulse-fed system in this study. In a completely mixed anaerobic tank acetate concentrations remain very low, and diffusion limitation will likely prevent Ca. Accumulibacter phosphatis microcolonies to grow out into larger granules. Especially for real wastewater, where only a limited amount of readily biodegradable COD is available for anaerobic conversion and storage, it is important to preferentially feed the largest granules. The challenge for stable granulation will be to design a system where, also under continuous feeding conditions, the readily biodegradable COD is directed preferentially to the largest granule fraction.

Interestingly we observed quite a difference in EBPR metabolism between the two feeding modes with respect to ratio of PAM/GAM metabolism and PHA remaining at the end of the aerated period. This is not well recognised yet in the literature and would need further attention. Our initial data seem to indicate that the bio-P removal capacity is not directly influenced, but the overall stability and response to disturbances (e.g. Monday effect) might be related to these differences (Brdjanovic et al., 1998; Rieger et al., 2001). Filipe et al. (2001b) indeed indicated that stabilising the feed to an EBPR process minimized disturbances, however the effect of different PAM/GAM metabolism was not yet well recognised and evaluated at the time. It might be relevant for the batch scheduling of the existing aerobic granular sludge facilities, for example.

5. Conclusion

An experimental study was performed at lab-scale to investigate the anaerobic contact mode of aerobic granular sludge with substrate on the distribution of substrate storage over the granule size fractions and the effects on sludge characteristics. Two reactors were operated identically, except for the anaerobic feeding phases. One reactor was fed from the bottom through the sludge bed, while the other was fed in a short pulse and subsequently mixed anaerobically. The following conclusions were derived from the observations.

- Bottom feeding primarily directs substrate towards the large granular size classes (i.e. large volume and closer to the bottom), while completely mixed pulse-feeding gives a more equal distribution of substrate over all granule sizes (i.e. surface area dependant).
- Both feeding methods resulted in stable granulation with large granules. However, in the completely mixed pulse-fed system the smaller granules are preferentially supplied with substrate due to their relatively higher surface-to-volume ratio. The preferential feeding of the larger granules in bottom-feeding will enhance and stabilise the granulation in such systems, certainly under less advantageous wastewater compositions then the acetate feed used in this study.
- The anaerobic contact mode directly impacts the substrate distribution over the different granule sizes, irrespective of the solids retention time of a granule as a unit.
- The systems showed very similar microbial populations with mainly *Ca.* Accumulibacter phosphatis present in the biomass. They differed strongly in their phenotype with respect to PAM/GAM metabolism, aerobic phosphate uptake rate, and residual PHA at the end of the aeration phase. These phenomena need attention in future EBPR studies since they are likely relevant for the full-scale stability of EBPR processes.

Funding

This work was funded by the Delfland Water Authority, Delfluent Services B.V., Evides Industriewater, the Rijnland District Water Control Board and Royal HaskoningDHV (all based in the Netherlands).

Declaration of Competing Interest

The authors declare that they have no known competing financial interests or personal relationships that could have appeared to influence the work reported in this paper.

Data availability

Data will be made available on request.

Acknowledgements

The authors would like to thank Roel van de Wijgaart for the sample preparation and microscopy performed in obtaining FISH-images and Jeffrey Croonenberg for the PHA analyses.

Supplementary materials

Supplementary material associated with this article can be found, in the online version, at doi:10.1016/j.watres.2023.119803.

References

- Acevedo, B., Oehmen, A., Carvalho, G., Seco, A., Borrás, L., Barat, R., 2012. Metabolic shift of polyphosphate-accumulating organisms with different levels of polyphosphate storage. Water Res. 46, 1889–1900. https://doi.org/10.1016/j. watres.2012.01.003.
- Amann, R.I., Binder, B.J., Olson, R.J., Chisholm, S.W., Devereux, R., Stahl, D.A., 1990.Combination of 16S rRNA-targeted oligonucleotide probes with flow cytometry for analyzing mixed microbial populations. Appl. Environ. Microbiol. 56, 1919.
- Bassin, J.P., Pronk, M., Muyzer, G., Kleerebezem, R., Dezotti, M., van Loosdrecht, M.C. M., 2011. Effect of elevated salt concentrations on the aerobic granular sludge process: linking microbial activity with microbial community structure. Appl. Environ. Microbiol. 77, 7942–7953. https://doi.org/10.1128/AEM.05016-11.
- Beun, J.J., van Loosdrecht, M.C.M., Heijnen, J.J., 2002. Aerobic granulation in a sequencing batch airlift reactor. Water Res. 36, 702–712. https://doi.org/10.1016/ S0043-1354(01)00250-0.
- Brdjanovic, D., Slamet, A., Van loosdrecht, M.C.M., Hooijmans, C.M., Alaerts, G.J., Heijnen, J.J., 1998. Impact of excessive aeration on biological phosphorus removal from wastewater. Water Res. 32, 200–208. https://doi.org/10.1016/S0043-1354 (97)00183-8.
- Brdjanovic, D., Nielsen, P.H., Lopez-Vazquez, C.M., van Loosdrecht, M.C.M. (Eds.), 2016.
 Experimental Methods in Wastewater Treatment. IWA Publishing. https://doi.org/ 10.2166/9781780404752.
- Crocetti, G.R., Hugenholtz, P., Bond, P.L., Schuler, A., Keller, J., Jenkins, D., Blackall, L. L., 2000. Identification of polyphosphate-accumulating organisms and design of 16S rRNA-directed probes for their detection and quantitation. Appl. Environ. Microbiol. 66, 1175–1182. https://doi.org/10.1128/AEM.66.3.1175-1182.2000.
- Crocetti, G.R., Banfield, J.F., Keller, J., Bond, P.L., Blackall, L.L., 2002. Glycogen-accumulating organisms in laboratory-scale and full-scale wastewater treatment processesbbThe GenBank accession numbers for the sequences reported in this paper are given in Methods. Microbiology 148, 3353–3364. https://doi.org/10.1099/00221287-148-11-3353
- Cussler, E.L., 2009. Diffusion: mass transfer in fluid systems. Cambridge Series in Chemical Engineering, 3rd ed. Cambridge University Press, Cambridge. https://doi. org/10.1017/CB09780511805134.
- Daims, H., Brühl, A., Amann, R., Schleifer, K.-H., Wagner, M., 1999. The domain-specific probe EUB338 is insufficient for the detection of all bacteria: development and evaluation of a more comprehensive probe set. Syst. Appl. Microbiol. 22, 434–444. https://doi.org/10.1016/S0723-2020(99)80053-8.
- De Kreuk, M.K., Van Loosdrecht, M.C.M.V., 2004. Selection of slow growing organisms as a means for improving aerobic granular sludge stability. Water Sci. Technol. 49, 9–17.
- Drewnowski, J., Makinia, J., 2011. The role of colloidal and particulate organic compounds in denitrification and EBPR occurring in a full-scale activated sludge system. Water Sci. Technol. 63. 318–324. https://doi.org/10.2166/wst.2011.056.
- Filipe, C.D.M., Daigger, G.T., Grady Jr, C.P.L., 2001. Stoichiometry and kinetics of acetate uptake under anaerobic conditions by an enriched culture of phosphorusaccumulating organisms at different pHs. Biotechnol. Bioeng. 76, 32–43. https://doi. org/10.1002/bit.1023.

Filipe, C.D.M., Meinhold, J., Jørgensen, S.-B., Daigger, G.T., Grady, C.P.L., 2001. Evaluation of the potential effects of equalization on the performance of biological phosphorus removal systems. Water Environ. Res. 73, 276–285. https://doi.org/ 10.2175/106143001X139281.

- Gjaltema, A., Tijhuis, L., van Loosdrecht, M.C.M., Heijnen, J.J., 1995. Detachment of biomass from suspended nongrowing spherical biofilms in airlift reactors. Biotechnol. Bioeng. 46, 258–269. https://doi.org/10.1002/bit.260460309.
- V.A. Haaksman, M. Mirghorayshi, M.C.M. van Loosdrecht, M. Pronk, Impact of aerobic availability of readily biodegradable COD on morphological stability of aerobic granular sludge, Water Research, Volume 187, 2020, 116402, ISSN 0043-1354, https://doi.org/10.1016/j.watres.2020.116402.
- Henze, M., Gujer, W., Mino, T., van Loosdrecht, 2000. Activated Sludge Models ASM1, ASM2, ASM2d and ASM3.
- Johnson, K., Jiang, Y., Kleerebezem, R., Muyzer, G., van Loosdrecht, M.C.M., 2009. Enrichment of a mixed bacterial culture with a high polyhydroxyalkanoate storage capacity. Biomacromolecules 10, 670–676. https://doi.org/10.1021/bm8013796.
- Kent, T.R., Bott, C.B., Wang, Z.-W., 2018. State of the art of aerobic granulation in continuous flow bioreactors. Biotechnol. Adv. 36, 1139–1166. https://doi.org/ 10.1016/j.biotechadv.2018.03.015.
- Kuba, T., Van Loosdrecht, M.C.M., Murnleitner, E., Heijnen, J.J., 1997. Kinetics and stoichiometry in the biological phosphorus removal process with short cycle times. Water Res. 31, 918–928.
- Layer, M., Adler, A., Reynaert, E., Hernandez, A., Pagni, M., Morgenroth, E., Holliger, C., Derlon, N., 2019. Organic substrate diffusibility governs microbial community composition, nutrient removal performance and kinetics of granulation of aerobic granular sludge. Water Res. X 4, 100033. https://doi.org/10.1016/j. wwo.2019.100033
- Liu, Y., Liu, Y.-Q., Wang, Z.-W., Yang, S.-F., Tay, J.-H., 2005. Influence of substrate surface loading on the kinetic behaviour of aerobic granules. Appl. Microbiol. Biotechnol. 67, 484–488. https://doi.org/10.1007/s00253-004-1785-1.
- Martins, A.M.P., Heijnen, J.J., van Loosdrecht, M.C.M., 2004. Bulking sludge in biological nutrient removal systems. Biotechnol. Bioeng. 86, 125–135. https://doi. org/10.1002/bit.20029.
- Metcalf, E., 2013. Wastewater Engineering: Treatment and Reuse. McGraw-Hill Education.
- Morgenroth, E., Wilderer, P.A., 1999. Controlled biomass removal the key parameter to achieve enhanced biological phosphorus removal in biofilm systems. Water Sci. Technol. 39, 33–40. https://doi.org/10.2166/wst.1999.0321.
- Nicolella, C., Van Loosdrecht, M.C.M., Heijnen, J.J., 1998. Mass transfer and reaction in a biofilm airlift suspension reactor. Chem. Eng. Sci. 53, 2743–2753
- Oyserman, B.O., Noguera, D.R., del Rio, T.G., Tringe, S.G., McMahon, K.D., 2016. Metatranscriptomic insights on gene expression and regulatory controls in Candidatus Accumulibacter phosphatis. ISME J. 10, 810–822. https://doi.org/ 10.1038/ismei.2015.155.
- Pereboom, J.H.F., 1994. Size distribution model for methanogenic granules from full scale UASB and IC reactors. Water Sci. Technol. 30, 211–221. https://doi.org/ 10.2166/wst.1994.0613.
- Pronk, M., Abbas, B., Al-Zuhairy, S.H.K., Kraan, R., Kleerebezem, R., Van Loosdrecht, M. C.M., 2015. Effect and behaviour of different substrates in relation to the formation of aerobic granular sludge. Applied microbiology and biotechnology 99, 5257–5268.
- Pronk, M., de Kreuk, M.K., de Bruin, B., Kamminga, P., Kleerebezem, R., van Loosdrecht, M.C.M., 2015. Full scale performance of the aerobic granular sludge process for sewage treatment. Water Res. 84, 207–217. https://doi.org/10.1016/j. watres.2015.07.011.
- Redmond, E., Jalbert, M., Young, M., Faraj, R., Sturm, B., Downing, L., 2019. Full-scale continuous flow selective pressures for sludge granulation. In: Presented at the WEFTEC 2019 - 92nd Annual Water Environment Federation's Technical Exhibition and Conference, pp. 3490–3497.
- Rieger, L., Koch, G., Kühni, M., Gujer, W., Siegrist, H., 2001. The eawag bio-p module for activated sludge model no. 3. Water Res. 35, 3887–3903. https://doi.org/10.1016/ S0043-1354(01)00110-5.
- Rocktäschel, T., Klarmann, C., Ochoa, J., Boisson, P., Sørensen, K., Horn, H., 2015. Influence of the granulation grade on the concentration of suspended solids in the effluent of a pilot scale sequencing batch reactor operated with aerobic granular sludge. Sep. Purif. Technol. 142, 234–241. https://doi.org/10.1016/j. seppur.2015.01.013.
- Schuler, A.J., Majed, N., Bucci, V., Hellweger, F.L., Tu, Y., Gu, A.Z., 2011. Is the whole the sumof its parts? Agent-basedmodelling of wastewater treatment systems. Water Sci. Technol. 63, 1590–1598. https://doi.org/10.2166/wst.2011.218.
- Silva, L.G.D., Tomás-Martínez, S., Loosdrecht, M.C.M.V., Wahl, S.A., 2019. The environment selects: modeling energy allocation in microbial communities under dynamic environments. bioRxiv 689174. https://doi.org/10.1101/689174.
- Silva, L.G., Gamez, K.O., Gomes, J.C., Akkermans, K., Welles, L., Abbas, B., Loosdrecht, M.C.M.V., Wahl, S.A., 2020. Revealing the metabolic flexibility of Candidatus Accumulibacter phosphatis through redox cofactor analysis and metabolic network modeling. Appl. Environ. Microbiol. https://doi.org/10.1128/ AEM.00808-20.
- Smolders, G.J.F., Klop, J.M., van Loosdrecht, M.C.M., Heijnen, J.J., 1995. A metabolic model of the biological phosphorus removal process: I. Effect of the sludge retention time. Biotechnol. Bioeng. 48, 222–233. https://doi.org/10.1002/bit.260480309.
- Smolders, G.J.F., Meij, J.V.D., Loosdrecht, M.C.M.V., Heijnen, J.J., 1995. A structured metabolic model for anaerobic and aerobic stoichiometry and kinetics of the biological phosphorus removal process. Biotechnol. Bioeng. 47, 277–287. https:// doi.org/10.1002/bit.260470302.
- 2540SOLIDS, 2017. Standard Methods For the Examination of Water and Wastewater. https://doi.org/10.2105/SMWW.2882.030.

- Stewart, P.S., 2003. Diffusion in biofilms. J. Bacteriol. 185, 1485–1491. https://doi.org/ 10.1128/JB.185.5.1485-1491.2003.
- Strubbe, L., Pennewaerde, M., Baeten, J.E., Volcke, E.I.P., 2022. Continuous aerobic granular sludge plants: better settling versus diffusion limitation. Chem. Eng. J. 428, 131427 https://doi.org/10.1016/j.cej.2021.131427.
- Tijhuis, L., Benthum, W.A.J.V., Loosdrecht, M.C.M.V., Heijnen, J.J., 1994. Solids retention time in spherical biofilms in a biofilm airlift suspension reactor. Biotechnol. Bioeng. 44, 867–879. https://doi.org/10.1002/bit.260440802.
- Tykesson, E., Aspegren, H., Henze, M., Nielsen, P.H., Jansen, J.I.C., 2002. Use of phosphorus release batch tests for modelling an EBPR pilot plant. Water Sci. Technol. 45, 99–106. https://doi.org/10.2166/wst.2002.0097.
- van den Berg, L., Pronk, M., van Loosdrecht, M.C.M., de Kreuk, M.K., 2021. Density measurements of aerobic granular sludge. Environ. Technol. 0, 1–11. https://doi. org/10.1080/09593330.2021.2017492.
- van den Berg, L., van Loosdrecht, M.C.M., de Kreuk, M.K., 2021. How to measure diffusion coefficients in biofilms: a critical analysis. Biotechnol. Bioeng. 118, 1273–1285. https://doi.org/10.1002/bit.27650.
- van Dijk, E.J.H., Haaksman, V.A., van Loosdrecht, M.C.M., Pronk, M., 2022. On the mechanisms for aerobic granulation model based evaluation. Water Res. 216, 118365 https://doi.org/10.1016/j.watres.2022.118365.
- Vishniac, W., Santer, M., 1957. The thiobacilli. Bacteriol. Rev. 21, 195-213.
- Wanner, J., Ottová, V., Grau, P., 1987. Effect of an anaerobic zone on settleability of activated sludge. In: Ramadori, R. (Ed.), Biological Phosphate Removal from Wastewaters. Pergamon, pp. 155–164. https://doi.org/10.1016/B978-0-08-035592-4-50010-5

- Wei, S.P., Stensel, H.D., Quoc, B.N., Stahl, D.A., Huang, X., Lee, P.-H., Winkler, M.-K.H., 2020. Flocs in disguise? High granule abundance found in continuous-flow activated sludge treatment plants. Water Res. 115865 https://doi.org/10.1016/j. watres 2020.115865
- Weissbrodt, D.G., Maillard, J., Brovelli, A., Chabrelie, A., May, J., Holliger, C., 2014. Multilevel correlations in the biological phosphorus removal process: from bacterial enrichment to conductivity-based metabolic batch tests and polyphosphatase assays. Biotechnol. Bioeng. 111, 2421–2435. https://doi.org/10.1002/bit.25320.
- Welles, L., Tian, W.D., Saad, S., Abbas, B., Lopez-Vazquez, C.M., Hooijmans, C.M., van Loosdrecht, M.C.M., Brdjanovic, D., 2015. Accumulibacter clades Type I and II performing kinetically different glycogen-accumulating organisms metabolisms for anaerobic substrate uptake. Water Res. 83, 354–366. https://doi.org/10.1016/j. watres.2015.06.045.
- Welles, L., Abbas, B., Sorokin, D.Y., Lopez-Vazquez, C.M., Hooijmans, C.M., Loosdrecht, V., M, M.C., Brdjanovic, D., 2017. Metabolic Response of "Candidatus Accumulibacter Phosphatis" Clade II C to Changes in Influent P/C Ratio. Front. Microbiol. 7 https://doi.org/10.3389/fmicb.2016.02121.
- Winkler, M.-K.H., van Loosdrecht, M.C.M., 2022. Intensifying existing urban wastewater. Science 375, 377–378. https://doi.org/10.1126/science.abm3900.
- Winkler, M.K.H., Kleerebezem, R., Khunjar, W.O., de Bruin, B., van Loosdrecht, M.C.M., 2012. Evaluating the solid retention time of bacteria in flocculent and granular sludge. Water Res. 46, 4973–4980. https://doi.org/10.1016/j.watres.2012.06.027.
- Zeng, R.J., Loosdrecht, M.C.M.V., Yuan, Z., Keller, J., 2003. Metabolic model for glycogen-accumulating organisms in anaerobic/aerobic activated sludge systems. Biotechnol. Bioeng. 81, 92–105. https://doi.org/10.1002/bit.10455.